

# Global Compression Commander: Plug-and-Play Inference Acceleration for High-Resolution Large Vision-Language Models

Xuyang Liu<sup>1\*</sup>, Ziming Wang<sup>2</sup>, Junjie Chen<sup>1</sup>, Yuhang Han<sup>3</sup>, Yingyao Wang<sup>2</sup>, Jiale Yuan<sup>2</sup>, Jun Song<sup>2✉</sup>, Linfeng Zhang<sup>4</sup>, Siteng Huang<sup>5</sup>, Honggang Chen<sup>1✉</sup>

<sup>1</sup> Sichuan University, <sup>2</sup> Taobao & Tmall Group of Alibaba, <sup>3</sup> Independent Researcher, <sup>4</sup> Shanghai Jiao Tong University, <sup>5</sup> Zhejiang University

## Abstract

Large vision-language models (LVLMs) excel at visual understanding, but face efficiency challenges due to quadratic complexity in processing long multi-modal contexts. While token compression can reduce computational costs, existing approaches are designed for single-view LVLMs and fail to consider the unique multi-view characteristics of high-resolution LVLMs with dynamic cropping. Existing methods treat all tokens uniformly, but our analysis reveals that global thumbnails can naturally guide the compression of local crops by providing holistic context for informativeness evaluation. In this paper, we first analyze dynamic cropping strategy, revealing both the complementary nature between thumbnails and crops, and the distinctive characteristics across different crops. Based on our observations, we propose “Global Compression Commander” (*i.e.*, **GlobalCom<sup>2</sup>**), a novel plug-and-play token compression framework for HR-LVLMs. GlobalCom<sup>2</sup> leverages thumbnail as the “commander” to guide the compression of local crops, adaptively preserving informative details while eliminating redundancy. Extensive experiments show that GlobalCom<sup>2</sup> maintains over **90%** performance while compressing **90%** visual tokens, reducing FLOPs and peak memory to **9.1%** and **60%**.

**Code:** <https://github.com/xuyang-liu16/GlobalCom2>.

## 1 Introduction

By bridging visual encoders with large language models (LLMs) (Touvron et al. 2023; Yang et al. 2024), large vision-language models (LVLMs) (Liu et al. 2024a; Bai et al. 2023) have recently achieved remarkable progress. As LVLMs advance towards high-resolution image understanding (HR-LVLMs), dynamic cropping has emerged as a de facto standard, represents a high-resolution image as a global thumbnail combined with a set of local crops. While this enables models like LLaVA-NeXT (Liu et al. 2024b) and InternVL 3 (Zhu et al. 2025) to capture fine-grained details with vision encoding efficiency, it also introduces challenges with increased visual tokens and hierarchical visual context.

To enhance the efficiency of LVLMs, recent efforts have increasingly adopted token compression approaches (Cha et al. 2024; Shang et al. 2025), which reduce visual tokens

\*Work done during intern at Taobao & Tmall Group of Alibaba.

✉ Corresponding author.



Figure 1: Design philosophy of “global-to-local” guided token compression. GlobalCom<sup>2</sup> evaluates the *information richness* of local crops from a global perspective to preserve informative regions while removing redundant ones.

while preserving essential information. These architecture-agnostic methods achieve optimal efficiency-accuracy trade-offs and have proven effective for LVLM acceleration. However, these methods were primarily designed for traditional *single-view* architectures (the entire image in Figure 1 top). While the *multi-view* dynamic cropping approach enables more fine-grained visual understanding, it further increases the number of visual tokens and computational overhead.

However, directly applying existing token compression methods to HR-LVLMs overlooks **three critical issues**: (i) **Global context neglect**: Current methods disregard the crucial role of global thumbnails in extracting holistic context and guiding visual understanding (Figure 2). (ii) **Information richness disparity**: They fail to account for varying information density across different crops (Figure 3), resulting in performance gaps exceeding **5%** on high-resolution tasks when comparing the removal of most versus least informative crops. (iii) **Content-agnostic positional bias**: Inner-LLM question-aware compression methods (Chen et al. 2024b; Xing et al. 2025; Zhang et al. 2025) systematically allocate more tokens to later-positioned crops irrespective of their actual informative content (Figure 4), inducing severe multi-modal hallucinations under extreme compression (Table 1), with detailed analysis provided in Appendix (Fig-

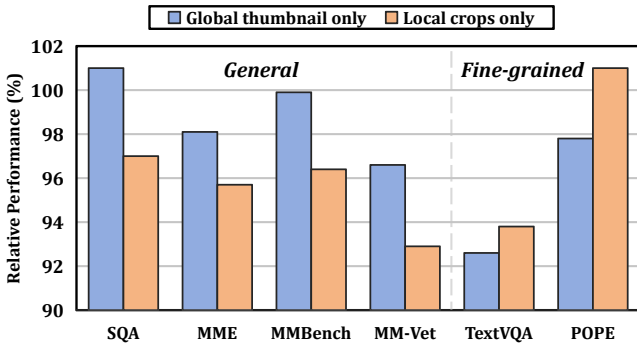


Figure 2: **Complementary roles of global thumbnail and local crops in HR-LVLMs with dynamic cropping.** Performance (%) denotes relative scores of LLaVA-NeXT-7B.

ure 9). These three oversights collectively result in **over-compression** of information-rich regions and disruption of the visual-semantic hierarchy (Figure 7).

To bridge this critical gap, we first conduct systematic analysis of dynamic cropping in Section 3, identifying *two key observations*: ❶ Thumbnail and crop tokens serve complementary roles - thumbnails capture holistic context while crops provide fine-grained details, enabling global importance evaluation. ❷ Through global context, tokens from different crops exhibit varying informativeness, requiring differentiated compression to minimize information loss.

Building on these observations, we propose “**Global Compression Commander**” (**GlobalCom<sup>2</sup>**), which follows a “*global-to-local*” guided token compression philosophy tailored for dynamic cropping-based HR-LVLMs. In Figure 1, GlobalCom<sup>2</sup> leverages holistic information from thumbnails to evaluate each crop’s information richness, adaptively adjusting compression intensity. It performs token compression through comprehensive evaluation from both global and local perspectives, achieving differentiated compression across regions while preserving significant information. This training-free approach extends seamlessly to video large language models (VideoLLMs) for efficient video understanding and can be integrated with existing question-aware methods. Notably, integrating this “global-to-local” design with FastV (Chen et al. 2024b) and SparseVLM (Zhang et al. 2025) achieves significant improvements of **5.3%** and **5.2%** across benchmarks while alleviating multi-modal hallucination caused by positional bias.

To summarize, our main contributions are three-fold:

- **Systematic Dynamic Cropping Analysis:** We empirically analyze the hierarchical nature of dynamic cropping and thoroughly investigate existing token compression methods for HR-LVLMs, identifying fundamental causes of critical information over-compression.
- **Global-to-Local Compression Philosophy:** We propose GlobalCom<sup>2</sup>, a training-free framework that adaptively adjusts compression intensity based on crop information richness assessment and preserves semantically important tokens across the entire visual hierarchy.
- **Superior Performance-Efficiency Trade-offs:** Extensive experiments on multiple HR-LVLMs and

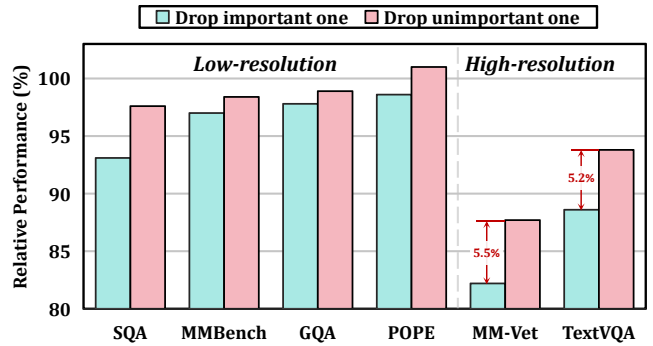


Figure 3: **Varying contributions of local crops.** Importance is quantified by the accumulated attention scores between thumbnail patches and [CLS] token within each crop.

VideoLLMs demonstrate exceptional balance of GlobalCom<sup>2</sup>, maintaining over 90% performance with 90% token reduction, while achieving substantial memory savings and throughput improvements.

## 2 Related Work

**High-resolution LVLMs.** Large vision-language models (LVLMs) integrate vision encoders and LLM decoders via projectors for feature alignment. Early LVLMs (Liu et al. 2024a; Bai et al. 2023) resize images to fixed resolutions, causing shape distortion and detail loss. To address this, high-resolution LVLMs have emerged in three categories: (i) Hybrid resolution methods using dual visual encoders (Li et al. 2024c; Luo et al. 2025). (ii) Native resolution methods with NaViT-style encoders (Wang et al. 2024; Guo et al. 2025). (iii) Dynamic cropping methods (Li et al. 2025; Zhu et al. 2025), which split images into regions for single-encoder processing. Dynamic cropping has gained widespread adoption (Lu et al. 2025; Chen et al. 2025) due to its vision encoding efficiency. However, increased visual tokens introduce computational challenges in inference speed and memory usage. Our work focuses on improving the efficiency of dynamic cropping-based HR-LVLMs.

**Token Compression for LVLMs.** Token compression has been widely adopted for LVLM acceleration through training-free approaches at two stages: (i) Vision Encoding stage (Shang et al. 2025; Yang et al. 2025): FasterVLM (Zhang et al. 2024) leverages [CLS] attention scores to prune visual tokens. (ii) LLM Pre-filling stage (Xing et al. 2025; Ye et al. 2025): FastV (Chen et al. 2024b) prunes tokens based on LLM self-attention, while SparseVLM (Zhang et al. 2025) uses cross-modal attention scores. Some methods combine both stages (Liu et al. 2024c). However, these methods treat all visual tokens equally in a “flat” token space, ignoring HR-LVLMs’ hierarchical structure where thumbnails and crops serve distinct roles.

Our work is the first to systematically quantify this oversight’s severe consequences, revealing critical failure modes including uniform over-compression and positional bias. We address this by proposing a “global-to-local” compression framework that leverages hierarchical structure, representing a shift toward structure-aware token compression.

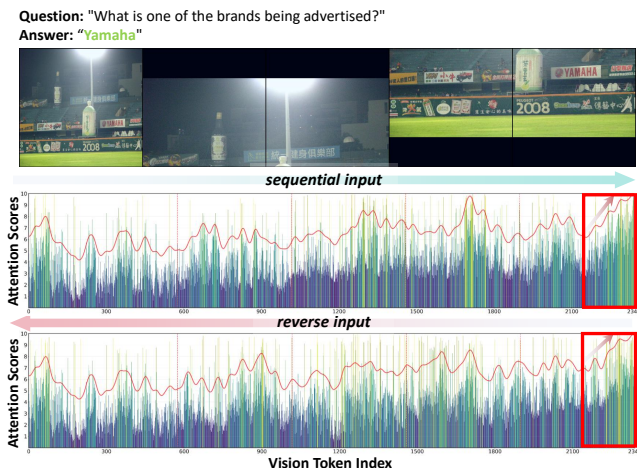


Figure 4: **Content-agnostic positional bias.** LLM attention-guided methods (e.g., FastV) assign higher scores (bars) to later tokens, regardless of their content or input order (second row: sequential crops; third row: reversed crops).

### 3 Analysis of Dynamic Cropping

#### 3.1 Preliminary

We take LLaVA-NeXT, a widely-adopted HR-LVLM with dynamic cropping, as an example to conduct our analysis.

**Model Architecture.** Given input image and text, LLaVA-NeXT generates responses through: (i) Vision Encoding: ViT (Radford et al. 2021) converts pixels to embeddings via MLP projector. (ii) LLM Decoding: LLM processes concatenated tokens, generating responses auto-regressively.

**Pre-processing.** LLaVA-NeXT uses grid templates:  $\{2 \times 2, 1 \times \{2, 3, 4\}, \{2, 3, 4\} \times 1\}$ . Images of size  $W \times H$  are scaled to  $(336 \times a) \times (336 \times b)$ , yielding  $n = a \times b$  local crops  $\mathbf{X}^L$  and a thumbnail  $\mathbf{X}^G$ . Total token length is  $(1 + n) \times N$ .

**Post-processing.** LLaVA-NeXT removes padding and adds boundary tokens to preserve aspect ratios.

#### 3.2 Stepping into Dynamic Cropping

HR-LVLMs process high-resolution images using dynamic cropping with thumbnails and crops. We analyze their characteristics to guide token compression design.

**(I) Functions of Thumbnail and Crops.** We investigate how thumbnail and crops contribute to image understanding in HR-LVLMs through experiments with LLaVA-NeXT-7B.

Figure 2 shows that thumbnail alone performs better on general visual perception tasks (e.g., SQA (Lu et al. 2022) and MMBench (Liu et al. 2024d)), benefiting from holistic visual information. In contrast, local crops excel in fine-grained tasks like text understanding (TextVQA (Singh et al. 2019)) and hallucination detection (POPE (Li et al. 2023)) by providing detailed features. Therefore, we identify that:

**Observation 1:** Global thumbnails and local crops serve complementary functions in HR-LVLMs with dynamic cropping: the former acts as a “comprehensive visual extractor” for holistic representations, while the latter serves as a “detailed visual capturer” for fine-grained representations.

**(II) Information Richness in Different Crops.** We investigate visual representation variance across crops through qualitative and quantitative analysis.

Figure 5 shows upper crops contain rich content (e.g., football players) while lower crops show mainly grass. CLIP-ViT’s last-layer attention distribution confirms higher semantic information in upper regions.

Quantitative experiments measuring crop importance via [CLS] attention scores and drop-crop tests on LLaVA-NeXT-7B (Figure 3) reveal substantial performance gaps: averaging 2.4% across benchmarks and reaching 5.5% and 5.2% on high-resolution tasks MM-Vet (Yu et al. 2024) and TextVQA (Singh et al. 2019) when dropping most versus least important crops. We thus identify:

**Observation 2:** Local crops exhibit varying information richness in global context, leading to different contributions to the overall visual understanding of HR-LVLMs with dynamic cropping, with visually informative crops being particularly crucial for capturing fine-grained local details.

### 4 Global Compression Commander

HR-LVLMs with dynamic cropping increase token length, making self-attention’s quadratic complexity a bottleneck. Inspired by human vision’s process of grasping scene gist before focusing on details, we propose “**Global Compression Commander**” (**GlobalCom<sup>2</sup>**) which implements a “global-to-local” compression strategy.

In Figure 5, for thumbnail token compression, we identify tokens with essential holistic information. Given the [CLS] token’s effectiveness as global image representation (Liang et al. 2022), GlobalCom<sup>2</sup> uses the last ViT layer’s attention map to compute attention between each token and [CLS]<sup>1</sup> (blue path in Figure 5). For the 1D token sequence  $\mathbf{X}^G$  of length  $N$ , the importance score  $s_i^G$  for the  $i$ -th token is:

$$s_i^G = \frac{\exp(\mathbf{q}^{\text{CLS}} \mathbf{K}_i^T / \sqrt{D})}{\sum_{i=1}^N \exp(\mathbf{q}^{\text{CLS}} \mathbf{K}_i^T / \sqrt{D})}, \quad (1)$$

where  $\mathbf{q}^{\text{CLS}}$  and  $\mathbf{K} \in \mathbb{R}^{N \times D}$  are query of [CLS] and keys of  $\mathbf{X}^G$ . Given a preset retention ratio  $R$  (%), GlobalCom<sup>2</sup> preserves the top- $k$  ( $k = R \times N$ ) tokens ranked by  $s_i^G$ :

$$\mathbf{X}^G \rightarrow \hat{\mathbf{X}}^G = \text{TopK}(\mathbf{X}^G, s_i^G, R \times N). \quad (2)$$

While thumbnail compression focuses on preserving holistic context, crop compression faces more complex challenges due to varying information densities across different crops. Following observation 2, semantically rich crops should preserve more tokens for crucial details, while less informative ones can be compressed more aggressively.

GlobalCom<sup>2</sup> leverages the comprehensive visual knowledge from thumbnails to guide crop compression through a decoupled two-stage process: (a) Adaptive Compression Adjustment, which dynamically adapts the compression intensity for each crop based on its information richness, and (b) Holistic Token Evaluation, which assesses the informativeness of tokens from both local and global views.

<sup>1</sup>For HR-LVLMs without [CLS] token, we propose an alternative token informativeness evaluation metric. See Appendix.

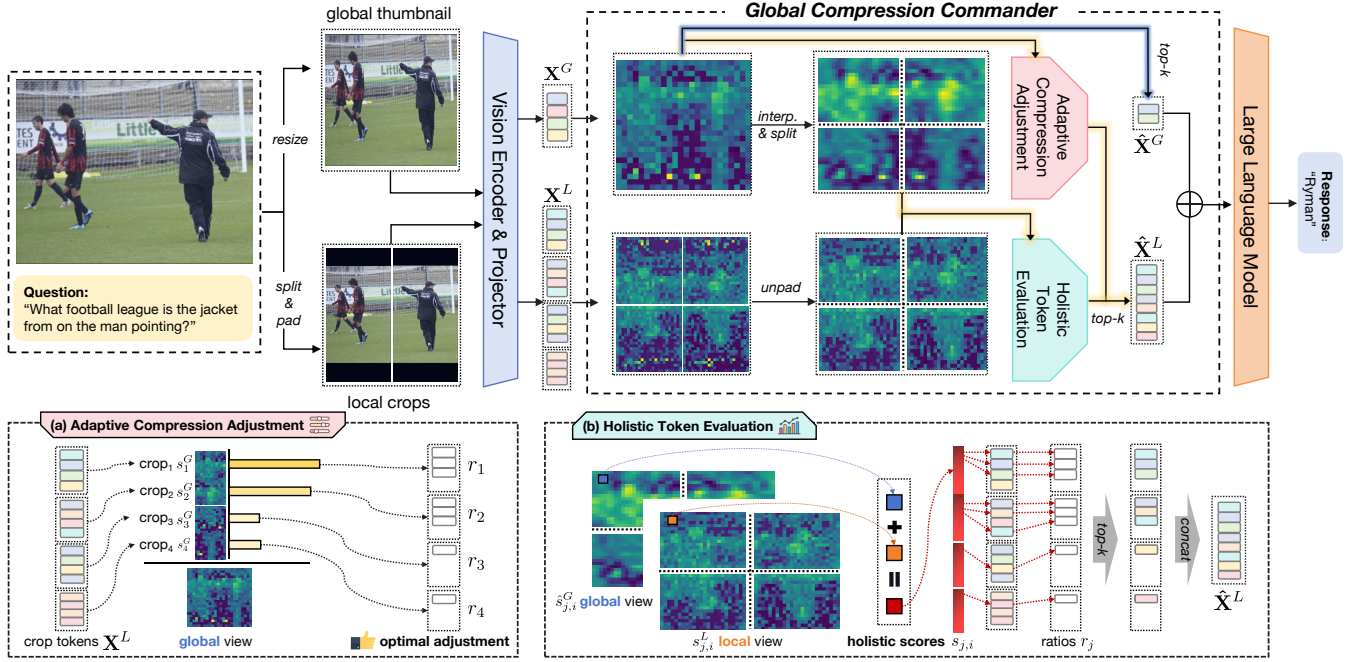


Figure 5: **Overall framework.** GlobalCom<sup>2</sup> guides token compression for HR-LVLMs through: 1) compressing thumbnail tokens (blue path), and 2) compressing crop tokens (yellow paths) by (a) adaptively adjusting compression intensity based on global visual richness, and (b) performing compression according to token informativeness from global and local perspectives.

#### 4.1 Adaptive Compression Adjustment

As shown in bottom-left of Figure 5, GlobalCom<sup>2</sup> analyzes each local crop’s semantic contribution and applies adaptive token compression accordingly.

For differentiated compression, we compute each crop’s *information richness score*  $s_j^G$  by accumulating patch-to-[CLS] attention scores in its corresponding global thumbnail region:  $s_j^G = \sum_{i \in \text{crop}_j} s_i^G$ . We then normalize scores with  $\tilde{s}_j = (s_j^G - \max(s_j^G)) / \tau$  ( $\tau = 10$ ) and compute relative importance weight  $\sigma_j$  via softmax:

$$\sigma_j = \frac{\exp(\tilde{s}_j)}{\sum_{l=1}^n \exp(\tilde{s}_l) + \epsilon}, \quad (3)$$

where  $\epsilon = 10^{-8}$  prevents division by zero. The final retention ratio  $r_j$  for each crop is adjusted from the preset ratio  $R(\%)$  based on its global content importance:

$$r_j = R \times \left(1 + \sigma_j - \frac{1}{n}\right), \quad (4)$$

where  $\sigma_j - \frac{1}{n}$  is deviation from average importance, allocating more tokens to important content and fewer to unimportant, for adaptive content-aware compression.

Through this process, GlobalCom<sup>2</sup> allocates compression degrees (i.e.,  $\{r_1, r_2, r_3, r_4\}$  in Figure 5) based on each crop’s information richness from the global view.

#### 4.2 Holistic Token Evaluation

After determining compression degrees for each crop, GlobalCom<sup>2</sup> evaluates token importance for preservation (Figure 5). For each crop, attention between patch tokens

and [CLS] yields *local importance scores*  $\{s_j^L\}_{j=1}^n$  from final-layer attention. These only capture within-crop importance, missing cross-region elements. Following observation ①, GlobalCom<sup>2</sup> incorporates global thumbnail context by reshaping 1D attention scores  $s_j^G$  to 2D format and applying bilinear interpolation to match original dimensions, yielding  $\{\hat{s}_j^G\}_{j=1}^n$  sub-maps per crop. The *holistic score*  $s_{j,i}$  for the  $i$ -th token in the  $j$ -th crop is:

$$s_{j,i} = \alpha \hat{s}_{j,i}^G + (1 - \alpha) s_{j,i}^L, \quad (5)$$

where we empirically set  $\alpha = 0.5$  to give equal consideration to both information sources (ablation study of  $\alpha$  is in Appendix Figure 10). The final compression:

$$\mathbf{X}_j^L \rightarrow \hat{\mathbf{X}}_j^L = \text{TopK}(\mathbf{X}_j^L, s_{j,i}, r_j \times N). \quad (6)$$

This holistic evaluation identifies globally significant tokens while preserving local details.

#### 4.3 Extension to Video Understanding

Given that VideoLLMs process sequential frames with substantial redundancy, analogous to HR-LVLMs with dynamic cropping, we extend GlobalCom<sup>2</sup> for efficient VideoLLMs. For video tokens  $\mathbf{V} = \{\mathbf{V}_j\}_{j=1}^T$ , we derive global representation  $\mathbf{v}^g$  via global average pooling. We compute cosine similarity between token  $i$  in frame  $j$  and  $\mathbf{v}^g$ :

$$s_{j,i}^G = -\text{sim}(\mathbf{v}_{j,i}, \mathbf{v}^g) = -\frac{\mathbf{v}_{j,i} \cdot \mathbf{v}^g}{\|\mathbf{v}_{j,i}\| \|\mathbf{v}^g\|}, \quad (7)$$

where global score  $s_{j,i}^G$  is negative cosine similarity, with lower similarity indicating higher distinctiveness. GlobalCom<sup>2</sup> calculates *information richness*  $s_j^G =$

Method	GQA	VizWiz	SQA	MMB	POPE	VQA <sup>T</sup>	MME	MM-Vet	Average
<i>Upper Bound, 2880 Tokens</i>									
LLaVA-NeXT-7B	64.2	57.6	70.1	67.4	86.5	64.9	1519.0	43.9	100.0%
<i>Ratio=50%, Retain up to 1440 Tokens</i>									
FastV <sub>(ECCV24)</sub>	61.8	54.9	69.0	67.4	85.5	59.6	1490.3	37.6	95.5%
PDrop <sub>(CVPR25)</sub>	63.7	<b>57.9</b>	<b>69.2</b>	<b>67.7</b>	87.9	61.6	1499.6	37.5	97.4%
SparseVLM <sub>(ICML25)</sub>	63.7	57.2	68.3	67.6	87.9	60.5	1507.2	36.8	96.8%
FasterVLM <sub>(2024.12)</sub>	63.4	56.4	69.1	67.4	87.7	58.9	1533.3	39.6	97.3%
<b>GlobalCom<sup>2</sup></b>	<b>63.9</b>	56.5	68.5	67.6	<b>88.1</b>	<b>62.3</b>	<b>1552.9</b>	<b>40.4</b>	<b>98.5%</b>
<i>Ratio=25%, Retain up to 720 Tokens</i>									
FastV <sub>(ECCV24)</sub>	60.4	54.2	<b>68.8</b>	65.6	83.1	58.4	1477.3	35.4	93.4%
PDrop <sub>(CVPR25)</sub>	60.3	<b>56.8</b>	68.5	65.6	85.5	59.8	1473.7	31.1	93.3%
SparseVLM <sub>(ICML25)</sub>	59.9	56.0	67.5	65.6	85.0	58.3	1465.9	38.5	94.6%
FasterVLM <sub>(2024.12)</sub>	61.3	55.4	67.1	<b>66.0</b>	87.2	58.8	1454.6	37.8	94.8%
<b>GlobalCom<sup>2</sup></b>	<b>61.5</b>	55.7	68.1	65.9	<b>87.6</b>	<b>60.9</b>	<b>1493.5</b>	<b>40.7</b>	<b>96.7%</b>
<i>Ratio=10%, Retain up to 288 Tokens</i>									
FastV <sub>(ECCV24)</sub>	55.9	53.1	68.1	61.6	71.7	55.7	1282.9	27.2	85.4%
PDrop <sub>(CVPR25)</sub>	54.5	54.4	67.7	59.0	77.6	54.4	1262.1	24.0	84.3%
SparseVLM <sub>(ICML25)</sub>	56.3	52.1	68.5	60.0	80.1	53.9	1334.2	26.5	86.1%
PruMerge <sub>(ICCV25)</sub>	53.6	54.0	66.4	61.3	60.8	50.6	1149.3	25.5	80.6%
FasterVLM <sub>(2024.12)</sub>	56.9	52.6	66.5	61.6	83.6	56.5	1359.2	35.0	89.9%
<b>GlobalCom<sup>2</sup></b>	<b>57.1</b>	<b>54.6</b>	<b>68.7</b>	<b>61.8</b>	<b>83.8</b>	<b>58.4</b>	<b>1365.5</b>	<b>36.4</b>	<b>91.6%</b>

Table 1: **Comparisons with LLaVA-NeXT across image understanding benchmarks.** VQA<sup>T</sup> (TextVQA), MME, MM-Vet are high-resolution benchmarks. ‘‘Average’’ shows mean performance across benchmarks, with **best** results highlighted.

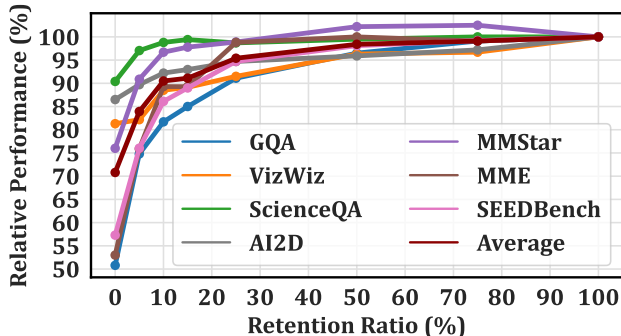


Figure 6: **Results of GlobalCom<sup>2</sup> on LLaVA-OneVision for image understanding.** GlobalCom<sup>2</sup> achieves 90.5% average performance with only 10% visual tokens.

$\sum_{i \in \text{frame}_j} s_{j,i}^G$  per frame. Following Equations 3-4, this guides compression intensity ( $r_j$ ), preserving more tokens in information-dense frames. For local importance, GlobalCom<sup>2</sup> generates frame representation  $\mathbf{v}_j^f$  through pooling and computes local scores  $s_{j,i}^L$  as negative cosine similarity. Combining both perspectives per Equation (5) yields *holistic score*  $s_{j,i}$ . Video compression is:

$$\mathbf{V}_j \rightarrow \hat{\mathbf{V}}_j = \text{TopK}(\mathbf{V}_j, s_j, r_j \times N). \quad (8)$$

Thus, GlobalCom<sup>2</sup> enables efficient VideoLLM inference through frame-wise adaptive compression.

## 5 Experiments

### 5.1 Experimental Setting

We evaluate on LLaVA-NeXT (Liu et al. 2024b) and LLaVA-OneVision (Li et al. 2025) for image understanding,

LLaVA-OneVision and Qwen2-VL (Wang et al. 2024) for video understanding. We compare with FastV (Chen et al. 2024b), SparseVLM (Zhang et al. 2025), PDrop (Xing et al. 2025), PruMerge (Shang et al. 2025), FasterVLM (Zhang et al. 2024), and VideoLLM methods DyCoke (Tao et al. 2025) and FrameFusion (Fu et al. 2025) at different retention ratios  $R$ . For fair comparison with multi-stage methods, we use ‘‘equivalent token count’’ reflecting the average percentage of vision tokens retained across all LLM layers.

### 5.2 Main Results

**Image Understanding.** Table 1 compares GlobalCom<sup>2</sup> with existing methods with LLaVA-NeXT, which demonstrates its three key advantages: **(i) Superior performance:** GlobalCom<sup>2</sup> consistently outperforms all baselines, being the only method that maintains **>90%** of the original performance across all retention ratios. **(ii) Extreme compression robustness:** While baseline methods suffer significant degradation at  $R = 10\%$ , GlobalCom<sup>2</sup> maintains robust performance and achieves the best results across all benchmarks, outperforming the second-best method by **1.7%** on average. Notably, FastV and PDrop demonstrate severe deterioration on POPE, exhibiting clear multi-modal hallucination due to positional bias from attention-guided token selection (Figure 7). **(iii) High-resolution excellence:** GlobalCom<sup>2</sup> demonstrates exceptional performance on high-resolution benchmarks (e.g., VQA<sup>T</sup>, MME, MM-Vet). Our ‘‘global-to-local’’ guided compression preserves both global semantics and local details, outperforming baselines that suffer from over-compression. Figure 6 further validates GlobalCom<sup>2</sup>’s effectiveness on LLaVA-OneVision, maintaining **90.5%** of the original performance at  $R = 10\%$  while consuming only **35.4%** of the original GPU memory.

Method	MVBench	LongVideoBench	MLVU	VideoMME			Average	
				Overall	Short	Medium		Long
<i>Upper Bound, 6272 Tokens</i>								
LLaVA-OneVision-7B	56.9	56.4	63.0	58.6	70.3	56.6	48.8	100.0%
<i>Ratio=30%, Retain 1882 Tokens</i>								
DyCoke (CVPR25)	56.6	54.7	60.3	56.1	67.1	54.6	46.6	96.5%
<i>Ratio=25%, Retain 1568 Tokens</i>								
FastV (ECCV24)	55.5	53.3	59.6	55.3	65.0	53.8	47.0	95.0%
PDrop (CVPR25)	55.3	51.3	57.1	55.5	64.7	53.1	48.7	94.2%
SparseVLM (ICML25)	56.4	53.9	60.7	57.3	68.4	55.2	48.1	97.5%
FrameFusion (ICCV25)	56.0	54.8	61.7	57.5	68.2	55.7	48.6	98.1%
<b>GlobalCom<sup>2</sup></b>	<b>57.0</b>	<b>55.4</b>	<b>62.6</b>	<b>58.1</b>	<b>69.2</b>	<b>55.8</b>	<b>49.4</b>	<b>99.3%</b>
<i>Ratio=15%, Retain 941 Tokens</i>								
FastV (ECCV24)	51.6	48.3	55.0	48.1	51.4	49.4	43.3	85.0%
PDrop (CVPR25)	53.2	47.6	54.7	50.1	58.7	48.7	45.0	87.4%
SparseVLM (ICML25)	52.9	49.7	57.4	53.4	61.0	52.1	47.0	91.2%
<b>GlobalCom<sup>2</sup></b>	<b>54.2</b>	<b>52.9</b>	<b>60.7</b>	<b>55.8</b>	<b>66.0</b>	<b>53.3</b>	<b>48.1</b>	<b>95.3%</b>

Table 2: **Comparisons with LLaVA-OneVision across video understanding benchmarks.** Each benchmark spans different durations: MVBench (16s), LongVideoBench (1-60min), MLVU (3-120min), and VideoMME-S/M/L (1-3/3-30/30-60min).

Method	LongVideo.MLVU		VideoMME			
	Overall	Short	Medium	Long		
<i>Upper Bound</i>						
Qwen2-VL-7B	56.0	60.4	57.6	70.0	54.6	48.2
<i>Ratio=25%</i>						
FastV (ECCV24)	Out of Memory (OOM)					
DyCoke (CVPR25)	50.5	55.2	51.5	62.1	47.1	45.1
<b>GlobalCom<sup>2</sup></b>	<b>51.4</b>	<b>55.9</b>	<b>54.3</b>	<b>64.7</b>	<b>50.1</b>	<b>48.2</b>

Table 3: **Comparisons on Qwen2-VL.** “LongVideo” is LongVideoBench. We conduct on 4 A100 GPUs.

Method	SQA	POPE	VQA <sup>T</sup>	MME	MM-Vet	Avg.
<i>Upper Bound, 2880 Tokens</i>						
Vanilla	70.1	86.5	64.9	1519.0	43.9	100.0%
<i>Ratio=25%, Retain up to 720 Tokens</i>						
Uniform	67.1	87.2	60.1	1454.6	37.8	94.2%
$\mathbf{n}_{\text{top-}k}$	67.4	87.3	59.8	1471.5	35.7	94.5%
Softmax (max)	67.3	87.2	60.3	1462.6	38.4	94.7%
<b>Softmax (sum)</b>	<b>67.6</b>	<b>87.4</b>	<b>60.6</b>	<b>1473.3</b>	<b>39.6</b>	<b>95.6%</b>

Table 4: **Effects of different adjustment strategies.** “Uniform” performs no compression adjustment, while the other three strategies enable adaptive compression adjustment.

See Appendix for results on the larger HR-LVLM.

**Video Understanding.** Table 2 presents GlobalCom<sup>2</sup>’s extension to video understanding with LLaVA-OneVision, demonstrating two key advantages: **(i) Superior VideoLLM performance:** GlobalCom<sup>2</sup> achieves **2.7%** average improvement over VideoLLM-specific method DyCoke (Tao et al. 2025) while using fewer vision tokens. **(ii) Advantages on long video understanding:** At  $R = 15\%$ , GlobalCom<sup>2</sup> achieves **3.2** and **3.3** points higher than the second-best method on LongVideoBench and MLVU, demonstrating the effectiveness of our “global-to-local” guided compression design. Table 3 shows GlobalCom<sup>2</sup> significantly outperforms DyCoke on Qwen2-VL, confirming its scalability. Additionally, FastV explicitly computes the full attention matrix in the certain layer, causing OOM issues with high token counts and limiting its practical applications.

Method	SQA	POPE	VQA <sup>T</sup>	MME	MM-Vet	Avg.
<i>Upper Bound, 2880 Tokens</i>						
Vanilla	70.1	86.5	64.9	1519.0	43.9	100.0%
<i>Ratio=25%, Retain up to 720 Tokens</i>						
Local only	67.6	87.4	60.6	1473.3	39.6	95.6%
Global only	67.9	86.4	60.2	1488.5	37.8	94.7%
<b>Global and Local</b>	<b>68.1</b>	<b>87.6</b>	<b>60.9</b>	<b>1493.5</b>	<b>40.7</b>	<b>96.7%</b>

Table 5: **Effects of different token evaluation metrics.** For the  $i$ -th token in crop  $j$ , “Global” and “Local” refer to importance scores  $\hat{s}_{j,i}^G$  and  $s_{j,i}^L$  in Equation (5), respectively.

### 5.3 Ablation Study and Analysis

**Ablation on Adaptive Compression Adjustment.** Table 4 compares four settings: (a) “Uniform” baseline with  $R = 25\%$  across all crops, and three adaptive strategies: (b) “ $\mathbf{n}_{\text{top-}k}$ ” adjusting compression based on top- $k$  most informative tokens per crop ( $k = 25\% \times N$ ), (c) “Softmax (max)” applying softmax over maximum token importance score  $s_j^G$  in each crop’s thumbnail, and (d) “Softmax (sum)” (our choice) computing softmax over sum of token importance scores  $s_j^G$  in each crop’s thumbnail region. All adaptive strategies outperform uniform compression, with “Softmax (sum)” achieving the best performance. While  $\mathbf{n}_{\text{top-}k}$  and “Softmax (max)” focus on strongest visual features per crop without considering global importance, “Softmax (sum)” adjusts compression based on each crop’s overall importance to the entire image, preserving more semantic information and helping the LLM capture finer visual details.

**Ablation on Holistic Token Evaluation.** Table 5 compares different token evaluation strategies. While both strategies are effective, each has limitations: Local-only evaluation excels at fine-grained tasks (VQA<sup>T</sup>, POPE) but underperforms on general perception benchmarks (MME, SQA) due to missing global context. Global-only evaluation maintains general perception but may overlook crucial local details. GlobalCom<sup>2</sup> achieves optimal performance by combining them, leveraging their complementary strengths.

**Combination with Question-aware Methods.** Figure 8 ex-

Q1: "What is the brand of this camera?"

A1: "DAKOTA DIGITAL"



Q2: "What brand is this drink?"

A2: "REDHOOK"

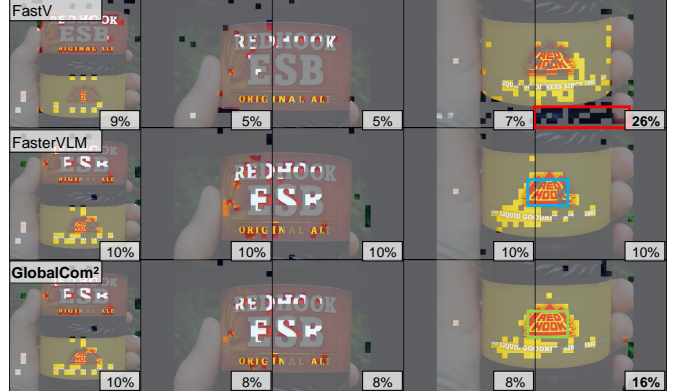


Figure 7: **Visualization of different token compression methods.** Gray masks indicate discarded tokens, where other methods exhibit significant *over-compression* issues, while GlobalCom<sup>2</sup> preserves both global important and local detailed information.

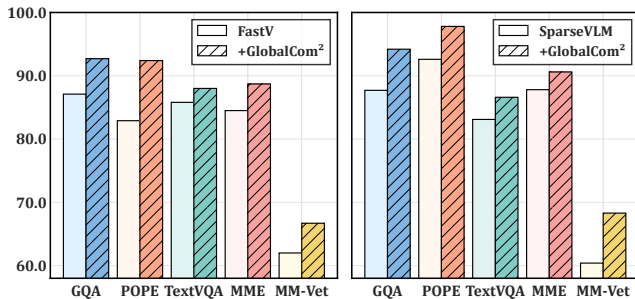


Figure 8: **Combination with question-aware methods.** “+GlobalCom<sup>2</sup>” indicates the application of our Adaptive Compression Adjustment strategy under  $R = 10\%$ .

plores combining GlobalCom<sup>2</sup> with question-aware methods FastV and SparseVLM, enabling joint consideration of *textual relevance and visual importance*. Using our Adaptive Compression Adjustment strategy, we assign optimal compression intensities (*i.e.*,  $r_j$  for the  $j$ -th crop) per crop based on its visual information richness within the global context before applying FastV/SparseVLM’s token evaluation metrics. Under extreme compression ( $R = 10\%$ ), incorporating GlobalCom<sup>2</sup> yields average improvements of **5.3%** and **5.2%** for FastV and SparseVLM. Notably, GlobalCom<sup>2</sup> significantly boosts performance on POPE, with improvements of **8.2** for FastV and **4.5** for SparseVLM, confirming our strategy’s effectiveness in *mitigating positional bias* by preventing over-compression of important regions.

#### 5.4 Efficiency Analysis

Table 6 compares inference efficiency among SparseVLM, FasterVLM and GlobalCom<sup>2</sup>. Unlike SparseVLM which requires explicit attention scores in LLM and is naturally incompatible with FlashAttention (Dao et al. 2022), FasterVLM and our GlobalCom<sup>2</sup> enable efficient computation before LLM decoding for efficient computation. As a plug-and-play solution, GlobalCom<sup>2</sup> achieves superior performance-efficiency trade-offs, maintaining **90%** of the original performance while dramatically reducing peak memory usage by **40%** and boosting inference throughput by  $1.8\times$ . Detailed analysis is in Appendix Table 10.

Method	FLOPs↓ (T)	Memory↓ (GB)	Throughput↑ (samples/s)	Performance↑
<i>Upper Bound, 2880 Tokens</i>				
Vanilla	41.7	23.0	3.8	100%
<i>Ratio=10%, Retain up to 288 Tokens</i>				
SparseVLM	5.4 ( $\downarrow 87.1\%$ )	24.2 ( $\uparrow 5.2\%$ )	5.9 ( $1.6\times$ )	85.7%
FasterVLM	<b>3.8</b> ( $\downarrow 90.9\%$ )	<b>13.6</b> ( $\downarrow 40.1\%$ )	<b>6.7</b> ( $1.8\times$ )	89.5%
<b>GlobalCom<sup>2</sup></b>	<b>3.8</b> ( $\downarrow 90.9\%$ )	<b>13.9</b> ( $\downarrow 40.0\%$ )	<b>6.7</b> ( $1.8\times$ )	<b>90.8%</b>

Table 6: **Efficiency comparisons.** “Memory”: peak GPU memory; “Throughput”: POPE samples/second; “Performance”: average score on eight multi-modal benchmarks.

#### 5.5 Compression Visualizations

Figure 7 compares compression processes of different methods at  $R = 10\%$  on VQA<sup>T</sup>, revealing over-compression issues in baselines: **(i) Positional Bias:** FastV exhibits clear positional bias, allocating more tokens ( $>3\times$ ) to later-positioned crops regardless of visual content. **(ii) Uniform Compression:** FasterVLM applies uniform compression across all crops, treating them as equally important. It fails to preserve critical information in some regions while retaining redundancy in others. In contrast, GlobalCom<sup>2</sup> globally assesses crop informativeness and adaptively adjusts compression ratios, preserving crucial details while eliminating redundancy. See Appendix Figure 11 for more examples.

## 6 Conclusion

Token compression has achieved significant progress in accelerating LLM inference. When applying existing methods to HR-LVLMs with dynamic cropping, these methods treat global thumbnails and local crops uniformly, overlooking their inherent characteristics. Through analyzing HR-LVLMs with dynamic cropping, we reveal distinct roles between thumbnails and crops, and observe varying information densities across crops. Based on these findings, we propose GlobalCom<sup>2</sup>, a plug-and-play token compression framework that operates on a “global-to-local” guided principle, adaptively preserving informative regions while minimizing redundancy. Experiments show that GlobalCom<sup>2</sup> achieves superior performance and efficiency across benchmarks, significantly outperforming existing baselines.

## References

- Bai, J.; Bai, S.; Yang, S.; Wang, S.; Tan, S.; Wang, P.; Lin, J.; Zhou, C.; and Zhou, J. 2023. Qwen-VL: A Frontier Large Vision-Language Model with Versatile Abilities. *arXiv preprint arXiv:2308.12966*.
- Cha, J.; Kang, W.; Mun, J.; and Roh, B. 2024. Honeybee: Locality-Enhanced Projector for Multimodal LLM. In *Proceedings of the IEEE/CVF Conference on Computer Vision and Pattern Recognition*, 13817–13827.
- Chen, G.; Li, Z.; Wang, S.; Jiang, J.; Liu, Y.; Lu, L.; Huang, D.-A.; Byeon, W.; Le, M.; Rintamaki, T.; et al. 2025. Eagle 2.5: Boosting long-context post-training for frontier vision-language models. *arXiv preprint arXiv:2504.15271*.
- Chen, L.; Li, J.; Dong, X.; Zhang, P.; Zang, Y.; Chen, Z.; Duan, H.; Wang, J.; Qiao, Y.; Lin, D.; and Zhao, F. 2024a. Are We on the Right Way for Evaluating Large Vision-Language Models? In *Proceedings of the Advances in Neural Information Processing Systems*.
- Chen, L.; Zhao, H.; Liu, T.; Bai, S.; Lin, J.; Zhou, C.; and Chang, B. 2024b. An Image is Worth 1/2 Tokens After Layer 2: Plug-and-Play Inference Acceleration for Large Vision-Language Models. In *Proceedings of the European Conference on Computer Vision*.
- Dao, T.; Fu, D. Y.; Ermon, S.; Rudra, A.; and Ré, C. 2022. FlashAttention: Fast and Memory-Efficient Exact Attention with IO-Awareness. In *Proceedings of the Advances in Neural Information Processing Systems*.
- Fu, C.; Chen, P.; Shen, Y.; Qin, Y.; Zhang, M.; Lin, X.; Qiu, Z.; Lin, W.; Yang, J.; Zheng, X.; Li, K.; Sun, X.; and Ji, R. 2023. MME: A Comprehensive Evaluation Benchmark for Multimodal Large Language Models. *arXiv preprint arXiv:2306.13394*.
- Fu, C.; Dai, Y.; Luo, Y.; Li, L.; Ren, S.; Zhang, R.; Wang, Z.; Zhou, C.; Shen, Y.; Zhang, M.; et al. 2024. Videomme: The first-ever comprehensive evaluation benchmark of multi-modal llms in video analysis. *arXiv preprint arXiv:2405.21075*.
- Fu, T.; Liu, T.; Han, Q.; Dai, G.; Yan, S.; Yang, H.; Ning, X.; and Wang, Y. 2025. FrameFusion: Combining Similarity and Importance for Video Token Reduction on Large Visual Language Models. In *Proceedings of the IEEE/CVF International Conference on Computer Vision*.
- Guo, D.; Wu, F.; Zhu, F.; Leng, F.; Shi, G.; Chen, H.; Fan, H.; Wang, J.; Jiang, J.; Wang, J.; et al. 2025. Seed1. 5-vl technical report. *arXiv preprint arXiv:2505.07062*.
- Gurari, D.; Li, Q.; Stangl, A. J.; Guo, A.; Lin, C.; Grauman, K.; Luo, J.; and Bigham, J. P. 2018. VizWiz Grand Challenge: Answering Visual Questions From Blind People. In *Proceedings of the IEEE/CVF Conference on Computer Vision and Pattern Recognition*, 3608–3617.
- Hudson, D. A.; and Manning, C. D. 2019. GQA: A New Dataset for Real-World Visual Reasoning and Compositional Question Answering. In *Proceedings of the IEEE/CVF Conference on Computer Vision and Pattern Recognition*, 6700–6709.
- Kembhavi, A.; Salvato, M.; Kolve, E.; Seo, M.; Hajishirzi, H.; and Farhadi, A. 2016. A diagram is worth a dozen images. In *Computer Vision—ECCV 2016: 14th European Conference, Amsterdam, The Netherlands, October 11–14, 2016, Proceedings, Part IV 14*, 235–251. Springer.
- Li, B.; Ge, Y.; Ge, Y.; Wang, G.; Wang, R.; Zhang, R.; and Shan, Y. 2024a. SEED-Bench: Benchmarking Multimodal Large Language Models. In *Proceedings of the IEEE/CVF Conference on Computer Vision and Pattern Recognition*, 13299–13308.
- Li, B.; Zhang, Y.; Guo, D.; Zhang, R.; Li, F.; Zhang, H.; Zhang, K.; Zhang, P.; Li, Y.; Liu, Z.; and Li, C. 2025. LLaVA-OneVision: Easy Visual Task Transfer. *Transactions on Machine Learning Research*.
- Li, K.; Wang, Y.; He, Y.; Li, Y.; Wang, Y.; Liu, Y.; Wang, Z.; Xu, J.; Chen, G.; Luo, P.; et al. 2024b. Mvbench: A comprehensive multi-modal video understanding benchmark. In *Proceedings of the IEEE/CVF Conference on Computer Vision and Pattern Recognition*, 22195–22206.
- Li, Y.; Du, Y.; Zhou, K.; Wang, J.; Zhao, W. X.; and Wen, J. 2023. Evaluating Object Hallucination in Large Vision-Language Models. In *Proceedings of the Conference on Empirical Methods in Natural Language Processing*, 292–305.
- Li, Y.; Zhang, Y.; Wang, C.; Zhong, Z.; Chen, Y.; Chu, R.; Liu, S.; and Jia, J. 2024c. Mini-Gemini: Mining the Potential of Multi-modality Vision Language Models. *arXiv preprint arXiv:2403.18814*.
- Liang, Y.; Ge, C.; Tong, Z.; Song, Y.; Wang, J.; and Xie, P. 2022. Not All Patches are What You Need: Expediting Vision Transformers via Token Reorganizations. In *Proceedings of the International Conference on Learning Representations*.
- Liu, H.; Li, C.; Li, Y.; and Lee, Y. J. 2024a. Improved Baselines with Visual Instruction Tuning. In *Proceedings of the IEEE/CVF Conference on Computer Vision and Pattern Recognition*, 26286–26296.
- Liu, H.; Li, C.; Li, Y.; Li, B.; Zhang, Y.; Shen, S.; and Lee, Y. J. 2024b. LLaVA-NeXT: Improved reasoning, OCR, and world knowledge.
- Liu, T.; Shi, L.; Hong, R.; Hu, Y.; Yin, Q.; and Zhang, L. 2024c. Multi-Stage Vision Token Dropping: Towards Efficient Multimodal Large Language Model. *arXiv preprint arXiv:2411.10803*.
- Liu, Y.; Duan, H.; Zhang, Y.; Li, B.; Zhang, S.; Zhao, W.; Yuan, Y.; Wang, J.; He, C.; Liu, Z.; Chen, K.; and Lin, D. 2024d. MMBench: Is Your Multi-modal Model an All-Around Player? In *Proceedings of the European Conference on Computer Vision*, 216–233.
- Lu, P.; Mishra, S.; Xia, T.; Qiu, L.; Chang, K.; Zhu, S.; Tafjord, O.; Clark, P.; and Kalyan, A. 2022. Learn to Explain: Multimodal Reasoning via Thought Chains for Science Question Answering. In *Proceedings of the Advances in Neural Information Processing Systems*, 2507–2521.
- Lu, X.; Chen, Y.; Chen, C.; Tan, H.; Chen, B.; Xie, Y.; Hu, R.; Tan, G.; Wu, R.; Hu, Y.; et al. 2025. Bluelm-v-3b: Algorithm and system co-design for multimodal large language

- models on mobile devices. In *Proceedings of the IEEE/CVF Conference on Computer Vision and Pattern Recognition*, 4145–4155.
- Luo, G.; Zhou, Y.; Zhang, Y.; Zheng, X.; Sun, X.; and Ji, R. 2025. Feast Your Eyes: Mixture-of-Resolution Adaptation for Multimodal Large Language Models. In *Proceedings of the International Conference on Learning Representations*.
- Radford, A.; Kim, J. W.; Hallacy, C.; Ramesh, A.; Goh, G.; Agarwal, S.; Sastry, G.; Askell, A.; Mishkin, P.; Clark, J.; Krueger, G.; and Sutskever, I. 2021. Learning Transferable Visual Models From Natural Language Supervision. In *Proceedings of the International Conference on Machine Learning*, 8748–8763.
- Shang, Y.; Cai, M.; Xu, B.; Lee, Y. J.; and Yan, Y. 2025. LLaVA-PruMerge: Adaptive Token Reduction for Efficient Large Multimodal Models. In *Proceedings of the IEEE/CVF International Conference on Computer Vision*.
- Singh, A.; Natarajan, V.; Shah, M.; Jiang, Y.; Chen, X.; Batta, D.; Parikh, D.; and Rohrbach, M. 2019. Towards VQA Models That Can Read. In *Proceedings of the IEEE/CVF Conference on Computer Vision and Pattern Recognition*, 8317–8326.
- Tao, K.; Qin, C.; You, H.; Sui, Y.; and Wang, H. 2025. DyCoke: Dynamic Compression of Tokens for Fast Video Large Language Models. In *Proceedings of the IEEE/CVF Conference on Computer Vision and Pattern Recognition*.
- Touvron, H.; Lavril, T.; Izacard, G.; Martinet, X.; Lachaux, M.; Lacroix, T.; Rozière, B.; Goyal, N.; Hambro, E.; Azhar, F.; Rodriguez, A.; Joulin, A.; Grave, E.; and Lample, G. 2023. LLaMA: Open and Efficient Foundation Language Models. *arXiv preprint arXiv:2302.13971*.
- Wang, P.; Bai, S.; Tan, S.; Wang, S.; Fan, Z.; Bai, J.; Chen, K.; Liu, X.; Wang, J.; Ge, W.; Fan, Y.; Dang, K.; Du, M.; Ren, X.; Men, R.; Liu, D.; Zhou, C.; Zhou, J.; and Lin, J. 2024. Qwen2-VL: Enhancing Vision-Language Model’s Perception of the World at Any Resolution. *arXiv preprint arXiv:2409.12191*.
- Wu, H.; Li, D.; Chen, B.; and Li, J. 2024. Longvideobench: A benchmark for long-context interleaved video-language understanding. In *Proceedings of the Advances in Neural Information Processing Systems*, volume 37, 28828–28857.
- Xing, L.; Huang, Q.; Dong, X.; Lu, J.; Zhang, P.; Zang, Y.; Cao, Y.; He, C.; Wang, J.; Wu, F.; et al. 2025. Pyramidrop: Accelerating your large vision-language models via pyramid visual redundancy reduction. In *Proceedings of the IEEE/CVF Conference on Computer Vision and Pattern Recognition*.
- Yang, A.; Yang, B.; Hui, B.; Zheng, B.; Yu, B.; Zhou, C.; Li, C.; Li, C.; Liu, D.; Huang, F.; Dong, G.; Wei, H.; Lin, H.; Tang, J.; Wang, J.; Yang, J.; Tu, J.; Zhang, J.; Ma, J.; Yang, J.; Xu, J.; Zhou, J.; Bai, J.; He, J.; Lin, J.; Dang, K.; Lu, K.; Chen, K.; Yang, K.; Li, M.; Xue, M.; Ni, N.; Zhang, P.; Wang, P.; Peng, R.; Men, R.; Gao, R.; Lin, R.; Wang, S.; Bai, S.; Tan, S.; Zhu, T.; Li, T.; Liu, T.; Ge, W.; Deng, X.; Zhou, X.; Ren, X.; Zhang, X.; Wei, X.; Ren, X.; Liu, X.; Fan, Y.; Yao, Y.; Zhang, Y.; Wan, Y.; Chu, Y.; Liu, Y.; Cui, Z.; Zhang, Z.; Guo, Z.; and Fan, Z. 2024. Qwen2 Technical Report. *arXiv:2407.10671*.
- Yang, S.; Chen, Y.; Tian, Z.; Wang, C.; Li, J.; Yu, B.; and Jia, J. 2025. VisionZip: Longer is Better but Not Necessary in Vision Language Models. In *Proceedings of the IEEE/CVF Conference on Computer Vision and Pattern Recognition*.
- Ye, W.; Wu, Q.; Lin, W.; and Zhou, Y. 2025. Fit and Prune: Fast and Training-free Visual Token Pruning for Multimodal Large Language Models. In *Proceedings of the AAAI Conference on Artificial Intelligence*.
- Yu, W.; Yang, Z.; Li, L.; Wang, J.; Lin, K.; Liu, Z.; Wang, X.; and Wang, L. 2024. MM-Vet: Evaluating Large Multimodal Models for Integrated Capabilities. In *Proceedings of the International Conference on Machine Learning*.
- Yuan, Z.; Shang, Y.; Zhou, Y.; Dong, Z.; Zhou, Z.; Xue, C.; Wu, B.; Li, Z.; Gu, Q.; Lee, Y. J.; Yan, Y.; Chen, B.; Sun, G.; and Keutzer, K. 2024. LLM Inference Unveiled: Survey and Roofline Model Insights. *arXiv preprint arXiv:2402.16363*.
- Zhai, X.; Mustafa, B.; Kolesnikov, A.; and Beyer, L. 2023. Sigmoid Loss for Language Image Pre-Training. In *Proceedings of the IEEE/CVF International Conference on Computer Vision*, 11941–11952.
- Zhang, Q.; Cheng, A.; Lu, M.; Zhuo, Z.; Wang, M.; Cao, J.; Guo, S.; She, Q.; and Zhang, S. 2024. [CLS] Attention is All You Need for Training-Free Visual Token Pruning: Make VLM Inference Faster. *arXiv preprint arXiv:2412.01818*.
- Zhang, Y.; Fan, C.-K.; Ma, J.; Zheng, W.; Huang, T.; Cheng, K.; Gudovskiy, D.; Okuno, T.; Nakata, Y.; Keutzer, K.; and Zhang, S. 2025. SparseVLM: Visual Token Sparsification for Efficient Vision-Language Model Inference. In *Proceedings of the International Conference on Machine Learning*.
- Zhou, J.; Shu, Y.; Zhao, B.; Wu, B.; Xiao, S.; Yang, X.; Xiong, Y.; Zhang, B.; Huang, T.; and Liu, Z. 2025. Mlvu: A comprehensive benchmark for multi-task long video understanding. In *Proceedings of the IEEE/CVF Conference on Computer Vision and Pattern Recognition*.
- Zhu, J.; Wang, W.; Chen, Z.; Liu, Z.; Ye, S.; Gu, L.; Tian, H.; Duan, Y.; Su, W.; Shao, J.; et al. 2025. Internvl3: Exploring advanced training and test-time recipes for open-source multimodal models. *arXiv preprint arXiv:2504.10479*.

## Appendix

In the appendix, we provide theoretical FLOPs calculation, more discussions about content-agnostic positional bias, GlobalCom<sup>2</sup> without [CLS] token, detailed benchmarks introduction and implementation details, more additional experiments and analysis, and detailed algorithm.

### A Theoretical Complexity Analysis

GlobalCom<sup>2</sup> compresses visual tokens for HR-LVLMs, thereby reducing their computational costs. Below, we analyze the theoretical computational complexity of HR-LVLMs in both the prefill stage and the decoding stage.

During the prefill stage, the FLOPs for a single transformer layer can be estimated using the formula  $8Td^2 + 4T^2d + 6Tdm$ . When applying a token retention ratio  $R$ , where the retained token count is defined as  $\hat{T} = R \cdot T$ , the corresponding theoretical FLOPs reduction ratio  $\eta$  can be reformulated to account for this adjustment:

$$\begin{aligned} \eta &= 1 - \frac{8\hat{T}d^2 + 4\hat{T}^2d + 6\hat{T}dm}{8Td^2 + 4T^2d + 6Tdm} \\ &= 1 - \frac{R(8d + 4RT + 6m)}{8d + 4T + 6m} \end{aligned} \quad (9)$$

In the decoding stage, the integration of a KV-Cache substantially enhances computational efficiency. This improvement is evidenced by the reduction in the complexity of attention computation to  $\mathcal{O}(T)$ . As a result, the formula for computing FLOPs is refined to  $8d^2 + 4Td + 6Tdm$ . Given the current limitations of hardware, managing dynamic KV-Cache lengths effectively during the inference process presents significant challenges. Therefore, implementing pruning strategies prior to the decoder in large language models could facilitate a more efficient acceleration of the inference process.

### B More Discussions about Content-agnostic Positional Bias.

Figure 9 reveals the inherent content-agnostic positional bias of the LLM attention-guided method FastV. Regardless of input order (sequential or reverse), FastV consistently assigns higher attention scores to later-positioned tokens when measuring visual token importance via LLM’s second-layer attention. In extreme compression settings ( $R = 10\%$ ), this bias causes severe over-compression—preserving later tokens while discarding potentially more informative earlier ones, resulting in sub-optimal performance and significant multi-modal hallucinations (14.8-point drop on POPE).

### C Discussions about LVLMs without [CLS].

Some Vision Encoders like SigLIP (Zhai et al. 2023) do not own [CLS] tokens, rendering existing token compression methods that rely on [CLS] tokens (e.g., FasterVLM (Zhang et al. 2024)) ineffective. Therefore, we explore alternative token importance evaluation approaches. This enables GlobalCom<sup>2</sup> to measure information content in

each crop and adaptively allocate token budgets, preserving tokens with higher **information richness**.

As visualized in Figure 12, we first examine the attention patterns of CLIP-ViT’s final layer [CLS] token as a baseline for evaluating alternative token importance assessment strategies. We explore two approaches to measure token information without relying on [CLS] token:

**(a) Patch Attention Analysis:** We calculate each patch token’s importance by averaging its attention scores with all other patch tokens:

$$a_i = \frac{1}{N-1} \sum_{j \neq i} A_{i,j}, \quad (10)$$

where  $A_{i,j}$  denotes the attention score from token  $i$  to token  $j$ , and  $N$  is the total number of patch tokens. Interestingly, as shown in the “Patch Attention” visualization in Figure 12, tokens with high informativeness exhibit **lower** average attention scores. This aligns with the intuition that tokens heavily attending to other tokens (high average attention scores) are more likely to be replaceable, as they primarily aggregate information from their neighbors. Conversely, tokens with low average attention scores tend to be more unique and irreplaceable, containing distinct information vital for image understanding. By negating these scores (shown as “Negative Patch Attention”), we obtain patterns that relatively align with [CLS]-based assessment.

**(b) Global Mean Similarity:** We compute a global mean vector  $\mathbf{g} \in \mathbb{R}^d$  through *global average pooling* over all tokens, then calculate the cosine similarity between each patch token  $\mathbf{x}_i$  and  $\mathbf{g}$ :

$$c_i = \text{sim}(\mathbf{x}_i, \mathbf{g}) = \frac{\mathbf{x}_i \cdot \mathbf{g}}{\|\mathbf{x}_i\| \|\mathbf{g}\|}, \quad (11)$$

Tokens with low similarity to  $\mathbf{g}$  typically represent **distinctive** visual elements that *deviate* from the average representation, suggesting their **irreplaceability** in capturing unique semantic information. Conversely, tokens highly similar to  $\mathbf{g}$  often correspond to common or repetitive patterns, indicating their redundancy in visual representation. The “Negative Similarity with token  $\mathbf{g}$ ” visualization aligns well with [CLS]-based assessment, highlighting semantically rich regions like the baseball player in the top-right example of Figure 12.

Based on these observations, we define two token importance measures:

$$s_i^{\text{attn}} = -a_i, \quad s_i^{\text{sim}} = -c_i, \quad (12)$$

where  $s_i^{\text{attn}}$  represents the “Negative Patch Attention” score and  $s_i^{\text{sim}}$  denotes the “Negative Similarity” score. Both scores are designed to highlight informative tokens:  $s_i^{\text{attn}}$  identifies tokens that maintain their distinctiveness by less attending to others, while  $s_i^{\text{sim}}$  emphasizes tokens that deviate from the average representation  $\mathbf{g}$ . These measures serve as effective alternatives to [CLS]-based assessment (denoted as  $s_i^{\text{[CLS]}}$ ) in our quantitative experiments.

Table 7 compares the effectiveness of  $s_i^{\text{[CLS]}}$ ,  $s_i^{\text{attn}}$ , and  $s_i^{\text{sim}}$  when used as metrics for both *adaptive compression adjustment* and *holistic token evaluation* in GlobalCom<sup>2</sup>.

Question: "What is one of the brands being advertised?"

Answer: "Yamaha"

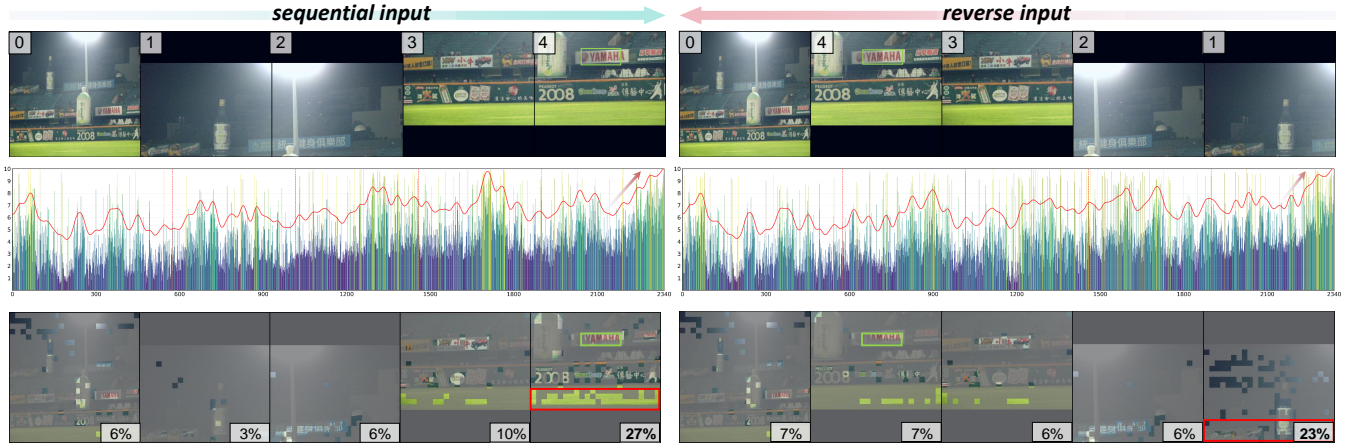


Figure 9: **Detailed analysis of content-agnostic positional bias.** LLM attention-guided methods (e.g., FastV (Chen et al. 2024b), PDrop (Xing et al. 2025)) assign disproportionately high scores (bars) to tokens in later positions, regardless of their actual semantic content or input order (second row: sequential crop input; third row: reverse crop input).

Method	VQA <sup>T</sup>	POPE	MME	MM-Vet	MMBSQA	Avg.
<i>Upper Bound, 2880 Tokens</i>						
Vanilla	64.9	86.5	1519.0	43.9	67.4	70.1
<i>Ratio=25%, Retain up to 720 Tokens</i>						
$s_i^{[CLS]}$	60.9	87.6	1493.5	39.5	65.9	68.1
$s_i^{attn}$	58.7	85.7	1449.3	36.6	63.5	67.9
$s_i^{sim}$	60.3	87.3	1485.8	39.7	65.0	67.6

Table 7: **Effects of different token evaluation metrics.**

While all three measures help preserve informative visual tokens to some extent,  $s_i^{attn}$  shows notably different behavior from the other two metrics. Notably,  $s_i^{sim}$  demonstrates performance closest to  $s_i^{[CLS]}$  across various benchmarks, even outperforming it on MM-Vet. Based on these results, we adopt  $s_i^{sim}$  as an alternative to  $s_i^{[CLS]}$  for measuring information content of local crops and visual tokens when [CLS] token is unavailable, enabling training-free token compression for HR-LVLMs.

## D Detailed Experimental Settings

**Benchmark Details.** We evaluate GlobalCom<sup>2</sup> on various multimodal understanding benchmarks detailed as follows:

- **GQA** (Hudson and Manning 2019): Contains 113,018 real-world images from Visual Genome with structured scene graphs for compositional visual reasoning. Features 22M diverse questions with functional program representations, focusing on multi-hop reasoning and semantic understanding with balanced answer distributions to reduce dataset biases.
- **VizWiz** (Gurari et al. 2018): Includes over 31,000 visual questions from blind users who took photos with phones and recorded spoken questions. Images are often poor quality due to lighting and framing issues, with conversational-style questions that may be unanswerable, representing real-world accessibility challenges.
- **SQA** (Lu et al. 2022): Contains 21,208 multimodal multiple-choice scientific questions from elementary and high school curricula, covering natural science, language science, and social science. Features 26 topics, 127 categories, and 379 different reasoning skills with detailed lectures (83.9%) and explanations (90.5%) for answers.
- **VQA<sup>T</sup>** (Singh et al. 2019): Features 28,408 high-resolution images from OpenImages with 45,336 questions focusing on reading and reasoning about text embedded in natural scenes. Requires OCR capabilities and text-based visual reasoning, with questions averaging 7.18 words in length.
- **A12D** (Kembhavi et al. 2016): Contains 5,000 high-resolution scientific diagrams from textbooks paired with 16,000 multiple-choice questions requiring visual-spatial reasoning about complex scientific concepts, processes, and relationships depicted in educational illustrations.
- **MMStar** (Chen et al. 2024a): Contains 1,500 challenging samples across 6 core capabilities (coarse perception, fine-grained perception, instance interaction, logical reasoning, science & technology, mathematics) designed to evaluate vision-indispensable reasoning without relying on shortcuts.
- **POPE** (Li et al. 2023): Features 3,000 images with 9,000 binary yes/no questions specifically designed for detecting object hallucination phenomena in large vision-language models. Uses systematic adversarial evaluation to probe model reliability and factual accuracy.
- **MME** (Fu et al. 2023): Contains 2,374 high-resolution images across 14 perceptual and cognitive reasoning subtasks, including existence, count, position, color, OCR, commonsense reasoning, numerical calculation, text translation, and code reasoning. Uses yes/no questions for comprehensive evaluation.
- **MMB** (Liu et al. 2024d): Features 2,974 multiple-choice questions designed for robust visual reasoning evaluation

across 20 ability dimensions including object localization, attribute recognition, scene understanding, and spatial relationship reasoning.

- **MMB-CN** (Liu et al. 2024d): Chinese counterpart of MMBench with 2,974 questions translated and culturally adapted for cross-lingual evaluation, maintaining the same 20 ability dimensions while incorporating Chinese cultural contexts and linguistic nuances.
- **MM-Vet** (Yu et al. 2024): Features 218 high-quality questions across 6 core VL capabilities (recognition, OCR, knowledge, language generation, spatial awareness, math) with complicated multi-modal reasoning chains requiring integration of multiple skills for comprehensive evaluation.
- **SEED-Bench** (Li et al. 2024a): Contains 19,242 human-annotated multiple-choice questions across 12 evaluation dimensions covering both image and video understanding tasks. Features hierarchical evaluation from basic perception to complex reasoning with balanced difficulty distribution.
- **MVBench** (Li et al. 2024b): Defines 20 video understanding tasks requiring deep temporal comprehension beyond single-frame analysis, including dynamic scene understanding, temporal action localization, multi-object tracking, and causal reasoning across video sequences.
- **LongVideoBench** (Wu et al. 2024): Focuses on long-context video understanding with 3,763 videos up to one hour duration and 6,678 questions across 17 categories including plot understanding, character analysis, temporal reasoning, and comprehensive video summarization.
- **MLVU** (Zhou et al. 2025): Features videos from 3 minutes to 2 hours with 9 tasks including topic reasoning, video summarization, needle-in-a-haystack retrieval, and ego-centric analysis, designed to evaluate long-form video comprehension and temporal memory capabilities.
- **VideoMME** (Fu et al. 2024): Comprises 900 videos and 2,700 questions across six domains (Knowledge, Film & Television, Sports, Life, Subtitles, Games) with durations from 11 seconds to 1 hour, featuring both with-subtitle and without-subtitle evaluation settings.

**Baseline Models.** We select LLaVA-NeXT (Liu et al. 2024b) and LLaVA-OneVision (SI) (Li et al. 2025) as our HR-LVLMs models, and follow the same inference setting as the original paper as it is publicly available<sup>2</sup>. LLaVA-NeXT and LLaVA-OneVision share a common three-component architecture: a pre-trained vision encoder, a large language model (LLM) backbone, and a two-layer MLP projector bridging the two. Specifically, LLaVA-NeXT employs CLIP-ViT-L-336px (Radford et al. 2021) and Vicuna-v1.5 for vision and language modeling respectively, while LLaVA-OneVision utilizes SigLIP-So400m-Patch14-384 (Zhai et al. 2023) and Qwen2 (Yang et al. 2024). To effectively process high-resolution visual inputs,

<sup>2</sup>LLaVA-NeXT: <https://github.com/haotian-liu/LLaVA/blob/main/docs/Evaluation.md>, LLaVA-OneVision: [https://github.com/LLaVA-VL/LLaVA-NeXT/blob/main/docs/LLaVA\\_OneVision.md](https://github.com/LLaVA-VL/LLaVA-NeXT/blob/main/docs/LLaVA_OneVision.md).

both models adopt flexible grid configurations - LLaVA-NeXT supports  $\{2 \times 2, 1 \times \{2, 3, 4\}, \{2, 3, 4\} \times 1\}$  with maximum  $5 \times 576$  grid tokens, while LLaVA-OneVision allows  $\{1 \times 1, \dots, 6 \times 6\}$  grids up to  $10 \times 729$  tokens. For hyperparameters,  $\tau$  and  $\alpha$  are respectively set as 10 and 0.5 for benchmark evaluations.

We also evaluate two VideoLLMs: LLaVA-OneVision and Qwen2-VL (Wang et al. 2024). LLaVA-OneVision unifies image and video tasks by encoding videos as long image-style token sequences, enabling strong zero-shot video understanding. Qwen2-VL adopts Naive Dynamic Resolution and Multimodal Rotary Position Embedding to achieve long video understanding (>20 min).

**Comparison Methods.** We compare our GlobalCom<sup>2</sup> with below dominant LVLM token compression methods:

- **FastV** (Chen et al. 2024b) performs one-time pruning after the selected LLM layer based on attention weights between vision tokens and the last token.
- **PDrop** (Xing et al. 2025) introduces progressive token dropping using similar token selection metrics as FastV, forming a pyramid-like token structure that balances efficiency and performance.
- **SparseVLM** (Zhang et al. 2025) ranks token importance by text-visual attention maps, pruning through pre-selected text prompts to reduce attention noise.
- **PruMerge** (Shang et al. 2025) integrates token pruning and merging by removing less important tokens using [CLS] attention weights with patch tokens and clustering retained tokens based on key similarity.
- **FasterVLM** (Zhang et al. 2024) re-ranks visual tokens by using [CLS] attention scores with all patch tokens from ViT and preserves top- $k$  tokens.

We also compare with two VideoLLM-specific methods:

- **DyCoke** (Tao et al. 2025) groups video frames using a four-frame sliding window and performs temporal token merging within each window.
- **FrameFusion** (Fu et al. 2025) adopts a two-stage strategy: first merging tokens across frames based on visual similarity, then selecting tokens within each frame based on importance.

All experiments in this work are conducted on NVIDIA A100-SXM4-80GB GPUs.

## E Additional Experiments

### E.1 Comparisons on LLaVA-NeXT-13B

Considering that both FasterVLM and GlobalCom<sup>2</sup> perform token compression at the vision encoding stage, Table 8 focuses on comparing these two methods on larger HR-LVLM LLaVA-NeXT-13B. The results reveal several key findings: **(i)** Our GlobalCom<sup>2</sup> outperforms FasterVLM on most benchmarks, maintaining **above 90%** of uncompressed performance across different retention ratios on both LLaVA-NeXT-7B and 13B models. **(ii)** On visual text understanding (VQA<sup>T</sup>), GlobalCom<sup>2</sup> shows particular strength at low retention ratios, surpassing FasterVLM by **2.3%** at  $R =$

Method	VQAv2	GQA	SQA	VQA <sup>T</sup>	POPE	MME	MMB	MMB-CN	Average
<i>Upper Bound, 2880 Tokens</i>									
LLaVA-NeXT-13B	82.8	65.4	73.5	67.1	86.2	1575.9	70.0	64.2	100.0%
<i>Ratio=75%, Retain up to 2160 Tokens</i>									
FasterVLM <sub>(2024.12)</sub>	<b>81.9</b>	64.6	72.6	62.8	87.6	1560.3	<b>69.8</b>	<b>64.8</b>	98.6%
<b>GlobalCom<sup>2</sup></b>	<b>81.9</b>	<b>65.0</b>	<b>72.8</b>	<b>65.2</b>	<b>87.8</b>	<b>1567.9</b>	69.2	64.7	<b>99.3%</b>
<i>Ratio=50%, Retain up to 1440 Tokens</i>									
FasterVLM <sub>(2024.12)</sub>	<b>81.3</b>	64.2	72.5	62.4	87.6	1534.1	<b>69.5</b>	<b>64.1</b>	97.5%
<b>GlobalCom<sup>2</sup></b>	81.0	<b>64.7</b>	<b>73.2</b>	<b>64.6</b>	<b>87.7</b>	<b>1553.5</b>	69.3	63.5	<b>98.4%</b>
<i>Ratio=25%, Retain up to 720 Tokens</i>									
FasterVLM <sub>(2024.12)</sub>	78.9	62.3	72.1	61.2	86.1	1516.1	67.6	62.1	95.3%
<b>GlobalCom<sup>2</sup></b>	<b>79.9</b>	<b>62.7</b>	<b>72.3</b>	<b>63.6</b>	<b>86.5</b>	<b>1531.2</b>	<b>67.9</b>	<b>62.2</b>	<b>96.1%</b>
<i>Ratio=10%, Retain up to 288 Tokens</i>									
FasterVLM <sub>(2024.12)</sub>	74.5	58.1	70.5	58.0	81.6	1386.2	61.7	53.5	88.6%
<b>GlobalCom<sup>2</sup></b>	<b>77.0</b>	<b>58.3</b>	<b>71.8</b>	<b>60.3</b>	<b>82.4</b>	<b>1399.5</b>	<b>65.0</b>	<b>58.5</b>	<b>90.9%</b>

Table 8: Comparison with FasterVLM on LLaVA-NeXT-13B across multiple benchmarks.

Method	GQA	VizWiz	SQA	AI2D	MMStar	MME	SEED	Avg.
<i>Upper Bound, 7290 Tokens</i>								
LLaVA-OV	59.5	46.0	67.9	54.2	36.2	1216.1	63.8	100.0%
$R = 75%$	58.9	44.5	67.9	52.7	37.1	1205.3	63.3	99.1%
$R = 50%$	57.4	44.3	67.6	52.0	37.0	1216.1	62.6	98.4%
$R = 25%$	54.2	42.1	67.0	51.3	35.8	1201.8	60.4	95.4%
$R = 15%$	50.6	41.0	67.5	50.4	35.4	1140.2	56.8	91.1%
$R = 10%$	48.6	40.7	67.1	50.0	35.0	1085.7	54.9	90.5%

Table 9: Results of GlobalCom<sup>2</sup> on LLaVA-OV-0.5B.

10%, thanks to its effective preservation of object and textual information. (iii) While FasterVLM performs slightly better on general visual tasks (VQAv2, MMB, MMB-CN) at high retention ratios due to its uniform token compression, GlobalCom<sup>2</sup> demonstrates superior degradation resistance at low ratios. For example, when  $R$  drops from 25% to 10%, FasterVLM’s performance significantly decreases by 5.9% and 8.6% on MMB and MMB-CN, while GlobalCom<sup>2</sup> only drops by 2.9% and 3.7%, benefiting from our carefully designed “global-to-local” guided compression strategy.

## E.2 Results on LLaVA-OneVision-0.5B

We adopt  $s_i^{sim}$  proposed in Section C as the measure for crop information richness and token informativeness, and evaluate our GlobalCom<sup>2</sup> on the LLaVA-OneVision model with more local crops across multiple benchmarks.

Results show that GlobalCom<sup>2</sup> maintains satisfactory performance even under low retention ratios ( $R = 25%, 15%, 10%$ ). Particularly, GlobalCom<sup>2</sup> achieves promising results on AI2D and MMStar benchmarks which involve high-resolution images. Interestingly, we observe that on the SQA benchmark, the model performance shows minimal degradation as token retention rate decreases. We attribute this to SQA’s lower dependency on visual signals and higher reliance on LLM capabilities. Given that LLaVA-OneVision employs the powerful Qwen2 (Yang et al. 2024) as its LLM decoder, it consistently performs well on this benchmark regardless of retention ratio.

## E.3 Sensitivity Analysis of Hyper-parameters

We further explore the hyper-parameter configurations  $\tau$  and  $\alpha$  of our GlobalCom<sup>2</sup> in Figure 10.

Hyper-parameter  $\tau$  serves as the temperature in the softmax function when assessing local crop significance, controlling the “sharpness” of probability distribution. A smaller  $\tau$  leads to a sharper distribution, amplifying the differences in global visual importance among local crops. As shown in the first row of Figure 10, our GlobalCom<sup>2</sup> demonstrates robust performance across most benchmarks, particularly on VQA<sup>T</sup> (Singh et al. 2019) and POPE (Li et al. 2023), with varying  $\tau$  validating our design principle for HR-LVLMs of allocating retention ratios based on each local crop’s global importance. We empirically set  $\tau = 10$  to achieve optimal performance across most benchmarks.

Hyper-parameter  $\alpha$  determines the criterion for token retention in local crops, where a larger  $\alpha$  indicates stronger dependence on global guidance for token retention in local crops. Similar to  $\tau$ , the second row of Figure 10 shows that our GlobalCom<sup>2</sup> exhibits consistent effectiveness across most benchmarks under different  $\alpha$  settings, substantiating our dual-perspective token retention strategy of local crops by considering their significance at both global and local levels for HR-LVLMs with dynamic cropping.

## E.4 Detailed Efficiency Analysis

We conduct a comprehensive analysis of both theoretical and practical efficiency of our GlobalCom<sup>2</sup> with LLaVA-NeXT-7B/13B on a single NVIDIA A100-SXM4-80GB GPU, as shown in Table 10. We measure computational efficiency using TFLOPs and peak memory consumption directly, while other metrics are estimated using LLM-Viewer (Yuan et al. 2024). Given that the sequence length of visual tokens substantially exceeds that of textual and system tokens, we *exclude* the latter two from our theoretical analysis. For practical efficiency, “Throughout” and the corresponding “Performance” measurements are conducted on the MME (Fu et al. 2023), which includes 2374 examples.

In Table 10, GlobalCom<sup>2</sup> substantially improves the computational efficiency of LLaVA-NeXT models across both

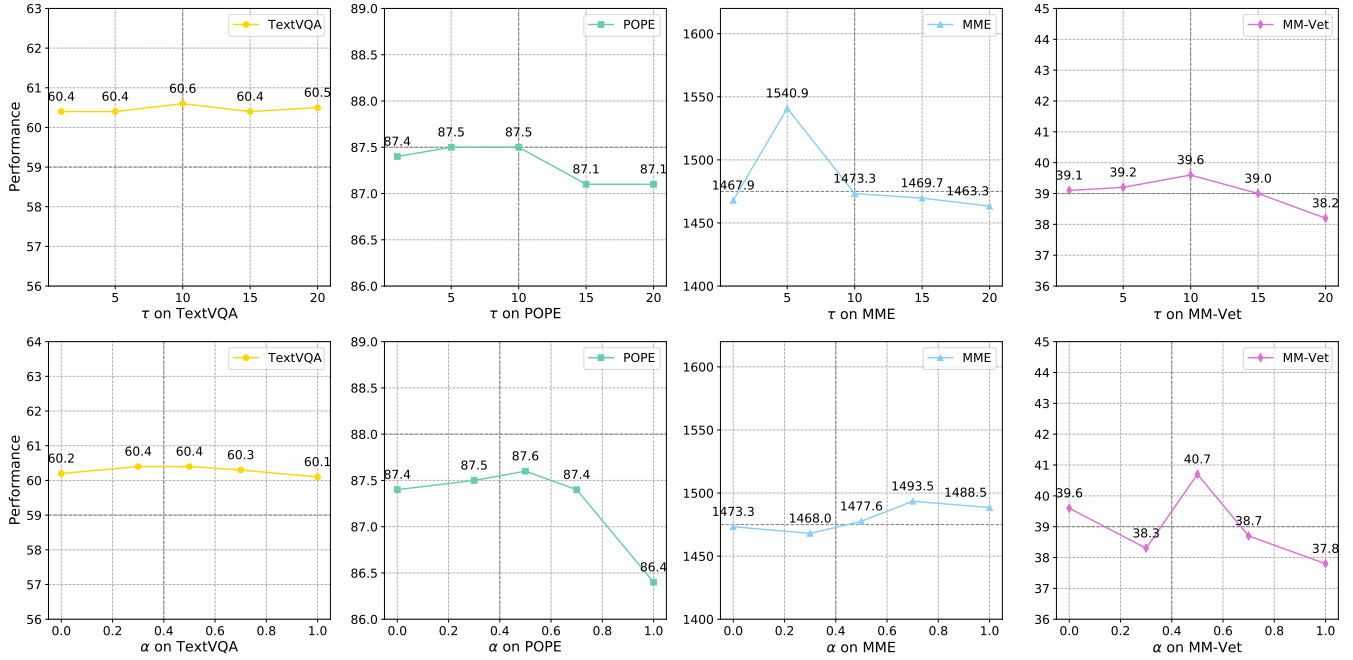


Figure 10: **Hyper-parameter sensitivity analysis of  $\tau$  and  $\alpha$ .** Hyper-parameter  $\tau$  controls the sharpness of probability distribution in softmax when assessing local crop informativeness. Hyper-parameter  $\alpha$  determines the token retention threshold where higher values indicate stronger reliance on global guidance.

Method	TFLOPs $\downarrow$	Peak Memory (GB) $\downarrow$	KV-Cache (MB) $\downarrow$	Prefill Time (ms) $\downarrow$	Throughput (samples/s) $\uparrow$	Performance $\uparrow$
<i>Upper Bound, 2880 Tokens</i>						
LLaVA-NeXT-7B	41.7	23.8	1536.0	170.7	2.5	1519.0
<i>Ratio=75%, Retain up to 2160 Tokens</i>						
<b>GlobalCom<sup>2</sup></b>	30.4 ( $\downarrow 27\%$ )	17.8 ( $\downarrow 25\%$ )	1126.4 ( $\downarrow 27\%$ )	119.9 ( $\downarrow 30\%$ )	3.2 (1.3 $\times$ )	1548.4
<i>Ratio=50%, Retain up to 1440 Tokens</i>						
<b>GlobalCom<sup>2</sup></b>	19.7 ( $\downarrow 53\%$ )	16.2 ( $\downarrow 32\%$ )	755.0 ( $\downarrow 51\%$ )	74.5 ( $\downarrow 57\%$ )	4.2 (1.7 $\times$ )	1552.9
<i>Ratio=25%, Retain up to 720 Tokens</i>						
<b>GlobalCom<sup>2</sup></b>	9.6 ( $\downarrow 77\%$ )	14.8 ( $\downarrow 39\%$ )	377.0 ( $\downarrow 76\%$ )	34.6 ( $\downarrow 80\%$ )	5.3 (2.1 $\times$ )	1493.5
<i>Ratio=10%, Retain up to 288 Tokens</i>						
<b>GlobalCom<sup>2</sup></b>	3.8 ( $\downarrow 91\%$ )	14.2 ( $\downarrow 40\%$ )	151.0 ( $\downarrow 90\%$ )	13.3 ( $\downarrow 92\%$ )	6.8 (2.7 $\times$ )	1365.5
<i>Upper Bound, 2880 Tokens</i>						
LLaVA-NeXT-13B	80.0	36.7	2457.6	295.1	1.9	1575.9
<i>Ratio=75%, Retain up to 2160 Tokens</i>						
<b>GlobalCom<sup>2</sup></b>	58.7 ( $\downarrow 27\%$ )	34.1 ( $\downarrow 7\%$ )	1843.2 ( $\downarrow 25\%$ )	211.6 ( $\downarrow 28\%$ )	2.4 (1.3 $\times$ )	1567.9
<i>Ratio=50%, Retain up to 1440 Tokens</i>						
<b>GlobalCom<sup>2</sup></b>	38.3 ( $\downarrow 52\%$ )	30.1 ( $\downarrow 18\%$ )	1228.8 ( $\downarrow 50\%$ )	134.6 ( $\downarrow 54\%$ )	3.2 (1.7 $\times$ )	1553.5
<i>Ratio=25%, Retain up to 720 Tokens</i>						
<b>GlobalCom<sup>2</sup></b>	18.7 ( $\downarrow 77\%$ )	27.5 ( $\downarrow 25\%$ )	590.0 ( $\downarrow 76\%$ )	64.1 ( $\downarrow 78\%$ )	4.8 (2.4 $\times$ )	1531.2
<i>Ratio=10%, Retain up to 288 Tokens</i>						
<b>GlobalCom<sup>2</sup></b>	7.4 ( $\downarrow 91\%$ )	26.2 ( $\downarrow 29\%$ )	236.0 ( $\downarrow 90\%$ )	25.0 ( $\downarrow 92\%$ )	5.8 (3.1 $\times$ )	1399.5

Table 10: **Comprehensive efficiency analysis with LLaVA-NeXT-7B/13B on one NVIDIA A100-SXM4-80GB GPU.**

theoretical and practical metrics. Specifically, while preserving model performance, our method achieves significant reductions in GPU memory consumption and notable acceleration in inference speed compared to the original model. Most importantly, these efficiency improvements are achieved through a training-free compression scheme, demonstrating its practical value.

## E.5 More Visualizations of Token Compression

In Figure 11, we present more token compression visualizations of GlobalCom<sup>2</sup>. It is clear that in all cases, *entity-rich* regions are effectively preserved while redundant ones are removed. For crops with high visual redundancy (e.g., the camera’s golden casing in the top-right case), it applies aggressive compression ( $r_4 = 19\%$ ). Conversely, for semantically dense regions (e.g., the text-rich first crop in the top-right case), it maintains more tokens ( $r_1 = 43\%$ ) to ensure

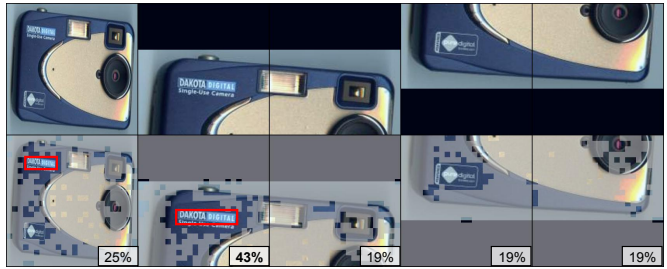
Q1: "What football league is the jacket from on the man pointing?"

A1: "Ryman"



Q2: "What is the brand of this camera?"

A2: "DAKOTA DIGITAL"



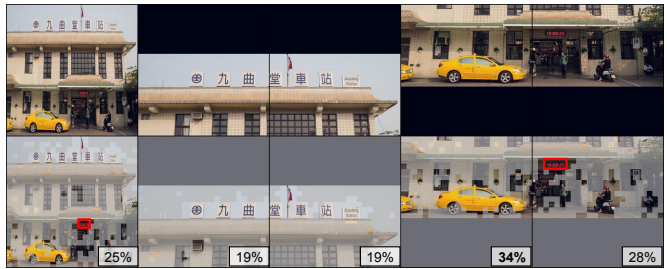
Q3: "What is the number of the runner in the lead right now?"

A3: "57859"



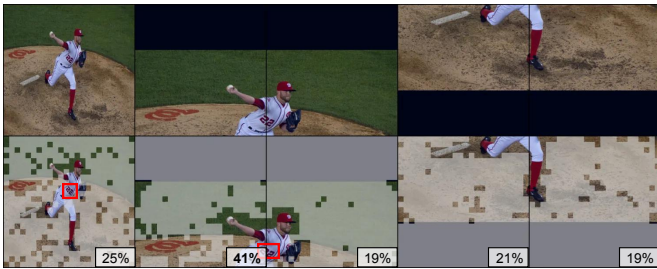
Q4: "What time is on the clock?"

A4: "15:08:25"



Q5: "What number is on the player's jersey?"

A5: "22"



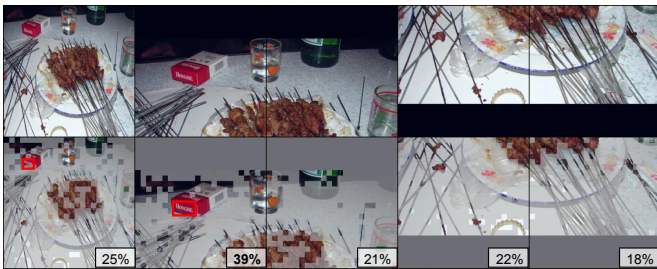
Q6: "Was the ruler made in 2002?"

A6: "Yes"



Q7: "What are the brand of cigarettes?"

A7: "Honghe"



Q8: "What number is the player looking at the children?"

A8: "9"



Figure 11: More visualization of token compression by GlobalCom<sup>2</sup>. The presented examples are from VQA<sup>T</sup>, where grey masks indicate discarded visual tokens.

detailed understanding. More cases in Appendix 11 further demonstrate GlobalCom<sup>2</sup>'s consistent ability to adaptively preserve significant regions while removing redundancy at both global and local views.

## F Algorithm Illustration

We present a comprehensive description of GlobalCom<sup>2</sup> token compression for both global thumbnail and local crops in Algorithm 1 and Algorithm 2, respectively.

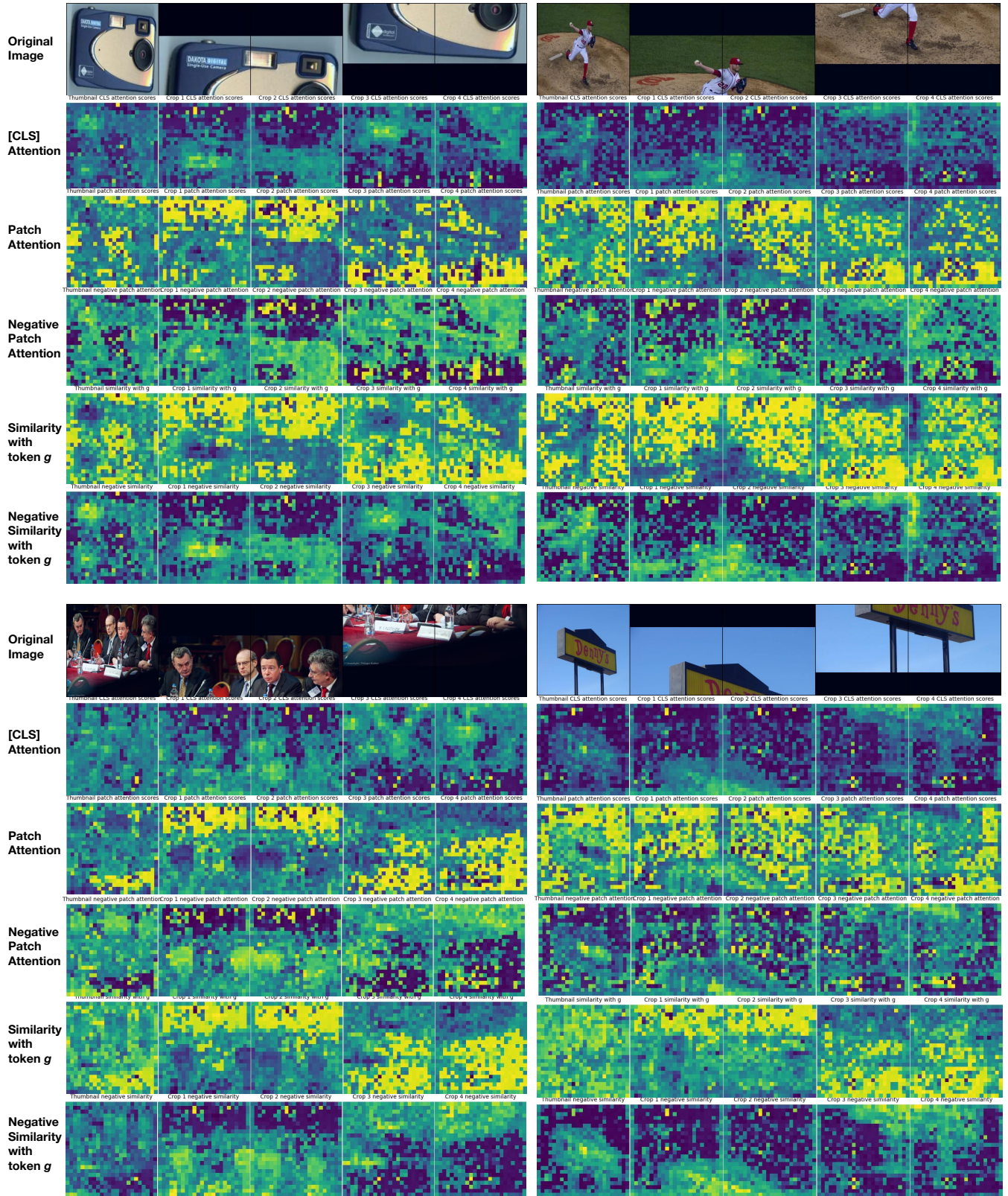


Figure 12: Visualization of different token evaluation scores.

---

**Algorithm 1: GlobalCom<sup>2</sup>: Thumbnail Compression**

---

**Require:** Global thumbnail tokens  $\mathbf{X}^G \in \mathbb{R}^{N \times D}$ , Vision encoder, Preset retention ratio  $R \in (0, 1]$

**Ensure:** Compressed tokens  $\hat{\mathbf{X}}^G \in \mathbb{R}^{k \times D}$  ( $k = R \cdot N$ )

- 1: // For models with [CLS] token
- 2: **if** model has [CLS] token **then**
- 3:     Get [CLS] query  $\mathbf{q}^{\text{CLS}}$  and Key matrix  $\mathbf{K}$
- 4:     Compute importance scores:

$$s_i^G \leftarrow \frac{\exp(\mathbf{q}^{\text{CLS}} \mathbf{K}_i^\top / \sqrt{D})}{\sum_{j=1}^N \exp(\mathbf{q}^{\text{CLS}} \mathbf{K}_j^\top / \sqrt{D})}, \forall i$$

- 5: **else**
- 6:     // For models without [CLS] token
- 7:     Compute global mean vector:  $\mathbf{g} \leftarrow \frac{1}{N} \sum_{i=1}^N \mathbf{x}_i$
- 8:     Compute cosine similarity scores:

$$s_i^G \leftarrow -\frac{\mathbf{x}_i \cdot \mathbf{g}}{\|\mathbf{x}_i\| \|\mathbf{g}\|}, \forall i$$

- 9: **end if**
  - 10: Sort indices:  $\text{idx} \leftarrow \text{argsort}([s_1^G, \dots, s_N^G])$  (descending)
  - 11: Retain top- $k$  tokens:  $\hat{\mathbf{X}}^G \leftarrow \mathbf{X}^G[\text{idx}[1 : k]]$
  - 12: **return**  $\hat{\mathbf{X}}^G$
- 

---

**Algorithm 2: GlobalCom<sup>2</sup>: Local Crop Compression**

---

**Require:** Local crops  $\{\mathbf{X}_j^L\}_{j=1}^n$ , Global importance scores  $s^G$ , Preset retention ratio  $R$ , Balance weight  $\alpha$ , Temperature  $\tau$

**Ensure:** Compressed crop tokens  $\{\hat{\mathbf{X}}_j^L\}_{j=1}^n$

- 1: **Adaptive Compression Adjustment:**
- 2: **for** each crop  $j \in [1, n]$  **do**
- 3:     Compute information richness:

$$s_j^G \leftarrow \sum_{i \in \text{crop}_j} s_i^G$$

- 4:     Normalize:  $\tilde{s}_j \leftarrow (s_j^G - \max\{s_j^G\}) / \tau$
- 5: **end for**
- 6: Compute importance weights:

$$\sigma_j \leftarrow \frac{\exp(\tilde{s}_j)}{\sum_{l=1}^n \exp(\tilde{s}_l) + \epsilon}$$

- 7: Adjust retention ratios:

$$r_j \leftarrow R \times \left(1 + \sigma_j - \frac{1}{n}\right)$$

- 8: **Holistic Token Evaluation:**
  - 9: **for** each crop  $j \in [1, n]$  **do**
  - 10:     Compute local scores  $s_j^L$  via vision encoder
  - 11:     Get global sub-scores  $\hat{s}_j^G$  via interpolation
  - 12:     L2-normalize both  $s_j^L$  and  $\hat{s}_j^G$
  - 13:     Combine scores:  $s_{j,i} \leftarrow \alpha \hat{s}_{j,i}^G + (1 - \alpha) s_{j,i}^L$
  - 14:     Compress:  $\hat{\mathbf{X}}_j^L \leftarrow \text{TopK}(\mathbf{X}_j^L, s_j, r_j \times N)$
  - 15: **end for**
  - 16: **return**  $\{\hat{\mathbf{X}}_j^L\}_{j=1}^n$
-